Bioconjugate Chemistry

Article

pubs.acs.org/bc

Dendrimer-Linked Antifreeze Proteins Have Superior Activity and Thermal Recovery

Corey A. Stevens,[†] Ran Drori,[‡] Shiran Zalis,[‡] Ido Braslavsky,[‡] and Peter L. Davies*[,†]

[†]Department of Biomedical and Molecular Sciences, Queen's University, Kingston, Ontario K7L 3N6, Canada

[‡]Institute of Biochemistry, Food Science and Nutrition, The Robert H. Smith Faculty of Agriculture, Food and Environment, The Hebrew University of Jerusalem, Rehovot 7610001, Israel

Supporting Information

ABSTRACT: By binding to ice, antifreeze proteins (AFPs) depress the freezing point of a solution and inhibit ice recrystallization if freezing does occur. Previous work showed that the activity of an AFP was incrementally increased by fusing it to another protein. Even larger increases in activity were achieved by doubling the number of ice-binding sites by dimerization. Here, we have combined the two strategies by linking multiple outward-facing AFPs to a dendrimer to significantly increase both the size of the molecule and the number of ice-binding sites. Using a heterobifunctional cross-linker, we attached between 6 and 11 type III AFPs to a second-generation polyamidoamine (G2-PAMAM) dendrimer with 16 reactive termini. This heterogeneous sample of dendrimer-linked type III constructs showed a greater than 4-fold increase in freezing point depression over that of monomeric type III AFP. This multimerized AFP was particularly effective at ice recrystallization inhibition activity, likely because it can simultaneously bind multiple ice surfaces. Additionally, attachment to the dendrimer has afforded the AFP superior recovery from heat denaturation. Linking AFPs together via polymers can generate novel reagents for controlling ice growth and recrystallization.

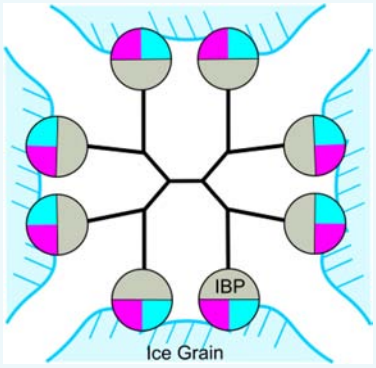

INTRODUCTION

Antifreeze proteins (AFPs) are produced by diverse overwintering organisms that are intolerant to freezing, such as fish and terrestrial insects.[1] In these animals, AFPs function by binding to any seed ice crystals that form internally to prevent their further growth and hence protect the organism from damage caused by freezing. The surface adsorption of AFPs to ice depresses the freezing temperature below the melting temperature, a phenomenon termed thermal hysteresis (TH). AFPs are also found in organisms, such as plants, that tolerate freezing.[2] Rather than blocking freezing, these AFPs function to prevent the growth (recrystallization) at high subzero temperatures of large ice crystals that would damage the frozen organism. This ability has led to use of AFPs in the frozen food industry to preserve product texture and improve storage.[3] The ability of AFPs and their mimic's to depress the freezing point of a solution has many possible applications in the health and biotechnology fields.[4−10] Advances in this area might be achieved by engineering these proteins to increase their freezing point depression and ice recrystallization inhibition (IRI) activities.

In tackling this objective, we sought to enhance AFP activity by attaching multiple copies of the protein onto a dendrimer.[11] Poly(amidoamine) (PAMAM) dendrimers are monodisperse, highly branched polymers suitable as a scaffold to generate compact protein multimers.[12] The attachment of multiple AFPs together via a dendrimer might also lead to improvements in solubility and stability.[13,14] One reason for anticipating activity enhancement stemmed from work done with type III AFP fusion proteins, where the 7 kDa AFP was fused via its N terminus to the much larger (42 kDa) maltose-binding protein. This bulky adduct proved that type III AFPs did not need to self-associate to form patches on the ice surface for antifreeze activity. Surprisingly, this simple size increase resulted in the fusion protein having more TH activity than that of the wild-type protein.[15] Subsequently, a series of type III AFP fusion proteins was analyzed and showed incremental increases in TH activity with increasing size of the fusion protein.[16]

Even greater increases in TH activity came from lengthening the ice-binding site (IBS) of an AFP, either in nature or as a result of protein engineering.[17,18] Engineering increases in IBS length require structural verification that the changes do not compromise the flatness, regularity, or functionality of the IBS. Similar gains in activity have resulted from generating AFP dimers, trimers, and tetramers that increase the number of IBSs rather than their length.[16,19−22] Here, by attaching multiple type III AFPs (6−11) to the outer termini of a dendrimer, termed dendrimer-linked type III AFP or DLTIII, we were able to enhance both TH and IRI activities. This was particularly evident at low multimer concentrations. In addition to increased activity, dendrimer linkage provided the AFP with enhanced recovery of activity following heat denaturation. The

Received: May 21, 2015
Revised: August 12, 2015
Published: August 12, 2015

DOI: 10.1021/acs.bioconjchem.5b00290
Bioconjugate Chem. 2015, 26, 1908−1915

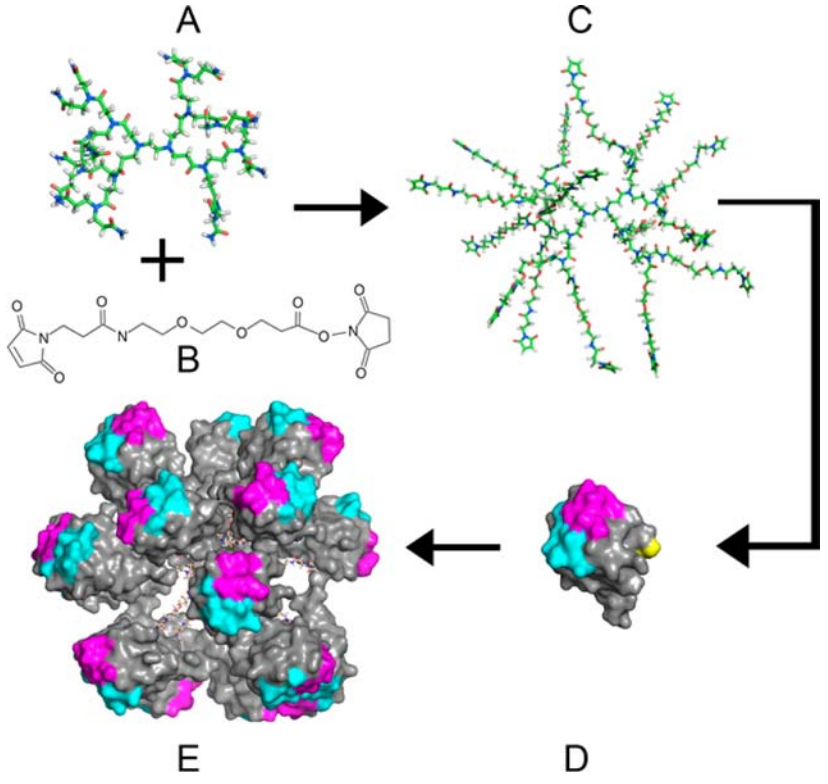

Figure 1. Schematic representation of the cross-linking reaction between G2-PAMAM dendrimer and type III antifreeze protein from ocean pout. (A) A second-generation polyamidoamine dendrimer (G2-PAMAM). (B) Heterobifunctional cross-linker SM(PEG)$_2$. (C) Model of a G2-PAMAM dendrimer fully decorated with 16 SM(PEG)$_2$ linkers. (D) Type III antifreeze protein from *Macrozoarces americanus* (ocean pout, PDB ID: 1HG7) with the compound ice-binding site colored in purple (pyramidal plane) and cyan (prism plane). The yellow coloring indicates the C-terminal cysteine residue (the His-tag sequence has been omitted). (E) Model of G2-PAMAM dendrimer with 16 type III antifreeze proteins populating the 16 arms.

combination of increased AFP size and multiple IBSs provides a novel way to improve both AFP activity and stability. Through the use of higher-order dendrimers and hyperactive AFPs, this approach has the potential to lead to even greater increases in AFP activity.

RESULTS

Assessment of Conjugation Reaction between AFP and Dendrimer. To attach multiple AFPs to the PAMAM dendrimer (Figure 1A) in a controlled manner, we used a heterobifunctional linker, SM(PEG)$_2$ (Figure 1B). The SM-(PEG)$_2$ linker has two reactive groups, *N*-hydroxysuccinimide (NHS) and maleimide, separated by a poly(ethylene glycol) (PEG) cross-bridge. The NHS-ester reacts specifically with primary amines, such as those of the dendrimer, to form a stable amide bond (Figure 1C). The maleimide group reacts with a reduced sulfhydryl on the protein (Figure 1D), forming a covalent thioether bond. The PEG cross-bridge increases solubility while serving to extend the proteins away from the dendrimer. Note that the location of A65C is the last residue of the C terminus of the AFP, which is on the opposite side of the protein from the IBS. So, after the cross-linking procedure, the IBSs of the linked AFPs should all be pointing outward, as shown by the model (Figure 1E). The efficacy of cross-linking was evaluated by SDS-PAGE analysis (Figure 2A). Control lanes consisting of dendrimer, SM(PEG)$_2$-modified dendrimer, and reduced type III A65C were run between the molecular weight markers (lane 1) and a sample from the conjugation reaction (lane 5). The sample of the conjugation reaction shows multiple distinct high-molecular-weight bands ranging from 60 to 125 kDa that were not present in the other lanes. Additionally, in the conjugation lane, the broad band near 7 kDa represents type III AFP not linked to the dendrimer and some disulfide bonded dimer at 14 kDa, which required separation from the AFP-bound dendrimer sample.

Purification of AFP-Linked Dendrimer. Unincorporated type III A65C was separated from dendrimer-linked type III AFPs (DLTIII) by size-exclusion chromatography under reducing conditions to prevent the formation of a disulfide bridge between type III AFP monomers (Figure 2B). Peak 1 in Figure 2B corresponds to the void volume of the column and does not contain significant amounts of DLTIII, as judged by SDS-PAGE (Figure 2C). Peak 2 has higher absorbance intensity than peak 3, but both show a similar high-molecular-weight banding patterns as that in lane 5 of the previous SDS-PAGE (Figure 2A). The fractions from the peaks 2 and 3 containing DLTIII were pooled and concentrated. Peak 4 corresponds to the large amount of unincorporated monomeric type III A65C (Figure 2C). The SDS-PAGE analysis provides an indication of purity and shows that size-exclusion chromatography was able to separate monomeric type III from the DLTIII.

Characterization of AFP−Dendrimer Multimers. Purified AFP−dendrimer conjugates were analyzed by MALDI-TOF to assess the number of AFP loaded onto the dendrimer (Figure 3). The reaction produced a heterogeneous mixture of conjugates, with the bulk of the material having a mass between 64.9 and 97.7 kDa, corresponding to between 6 and 11

DOI: 10.1021/acs.bioconjchem.5b00290
Bioconjugate Chem. 2015, 26, 1908−1915

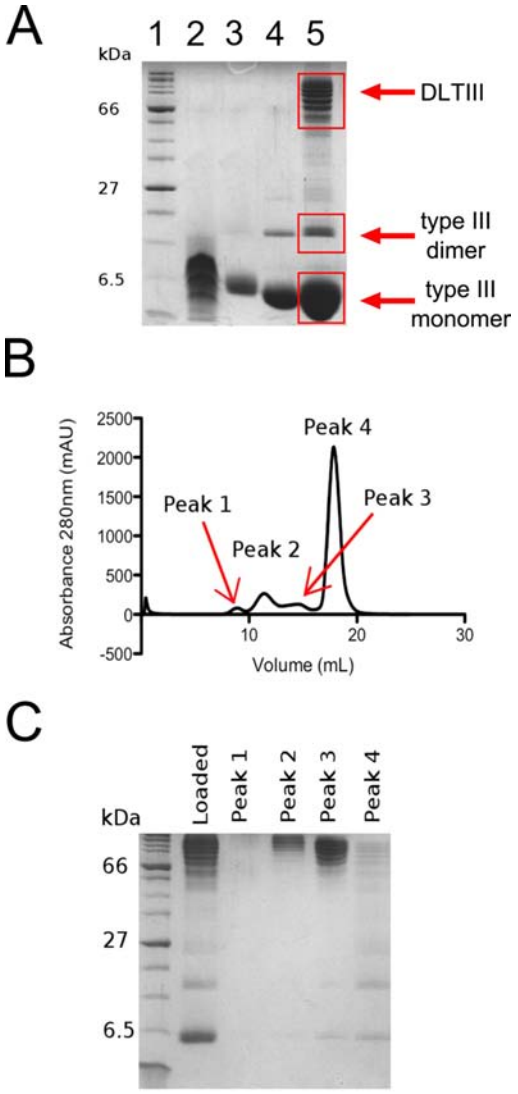

Figure 2. Assessment and purification of the cross-linking reaction between the G2-PAMAM dendrimer and type III antifreeze protein. (A) SDS-PAGE analysis of the cross-linking reaction run alongside various controls: 1, molecular weight marker; 2, G2-PAMAM dendrimer; 3, G2-PAMAM dendrimer reacted with heterobifunctional cross-linker; 4, type III A65C antifreeze protein; 5, result of the cross-linking reaction between heterobifunctional cross-linker-modified G2-PAMAM dendrimer and type III A65C antifreeze protein. (B) G75-Sephadex size-exclusion chromatography elution profile of the product from the cross-linking reaction. (C) SDS-PAGE analysis of selected fractions from the G75-Sephadex size-exclusion chromatography purification of dendrimer-linked type III (DLTIII).

attached AFPs per dendrimer. The apex of the broad peak at 73.4 kDa represents the mean of eight linked AFPs (Table 1). Linear regression analysis comparing predicted and observed molecular weights follows the equation $y = 0.97x + 1.81$, with an $R^2 = 0.998$ (Supporting Information Figure S4). A slope and R^2 value near 1 indicate the high level of accuracy with which the observed molecular weights match the predicted weights.

Thermal Hysteresis Activity and Ice Crystal Morphology. The ability of the dendrimer−AFP multimers to inhibit ice growth in aqueous medium was assessed by ice crystal morphology and TH. In the presence of DLTIII, ice crystals were shaped into hexagonal bipyramids characteristic of moderately active AFPs in general and type III AFP in particular.[23] Attaching type III AFP to the dendrimer did not affect ice crystal morphology, suggesting that the ice-binding site of type III AFP has not been altered or occluded. The heterogeneous mixture of DLTIII AFP molecules was extremely active in thermal hysteresis (Figure 4). For comparison, the TH activity of dendrimer-linked type III AFP (black line) was plotted against monomeric type III AFP (red line) and maltose-binding protein-linked type III AFP (blue line) based on molar amounts of each construct (Figure 4A).[15] When comparing the TH activities on a molar basis, increasing concentrations of each type III construct led to an increase in the amount of TH. The plots resembled rectangular hyperbolas but shifted to higher values for the larger constructs. At concentrations below 0.07 mM, the dendrimer showed a 4-fold increase in TH activity compared to that of the monomeric type III AFP. Furthermore, to assess activity on a per AFP-domain basis, we normalized the concentration of the DLTIII conjugate (black line) to monomeric type III AFP (red line, Figure 4B). This type of assessment indicates that the DLTIII conjugate has enhanced activity over monomeric type III at concentrations higher than 0.15 mM. We attempted to assay even higher concentrations of DLTIII, but we were unable to form a single ice crystal due to the high level of melting hysteresis.[24] Melting hysteresis is the elevation of the melting point due to the surface adsorption of AFPs. At high concentrations of DLTIII, adsorption of the molecule to ice led to superheating, which prevented the isolation of a single ice crystal for TH measurements.

Ice Recrystallization Inhibition Assessment of Dendrimer-Linked Type III AFP. IRI activity of DLTIII was assessed by two established techniques: the splat and sucrose-sandwich assays. The ability of the dendrimer−AFP molecule to prevent ice recrystallization as compared to that of monomeric type III was investigated by testing various dilutions with the splat assay (Figure 5A). At an initial concentration of 1.4 μM, both monomeric and dendrimer-linked type III AFPs are able to inhibit recrystallization, as indicated by the small ice grains after 16 h of recrystallization. A 2-fold dilution of the monomeric-type III AFP was enough to abolish IRI activity. However, a greater than 15-fold dilution was required to stop IRI by the DLTIII sample. This result indicates the dendrimer-linked AFP molecule is able to prevent recrystallization at lower molar concentrations than monomeric type III AFP. However, on the basis of the number of AFPs being directly compared, free or bound, the samples are equally effective. Another point of interest is the differences in the ice grain boundaries between the two samples. Recrystallization in the presence of low amounts of monomeric type III (or no AFP; Supporting Information Figure S2) led to the formation of regularly shaped and ordered ice crystals with crisp grain boundaries. However, low concentrations of DLTIII caused irregularly shaped ice grains to form with indistinct boundaries, suggesting that the channels between ice grains are narrowed (Figure 5A, 0.08 μM enlargements).

A striking result was seen with the sucrose-sandwich assay (Figure 5B). When recrystallization occurred in the absence of AFPs, or at very low AFP concentrations, ice crystals expanded and contracted in the shape of uniform discs (Figure 5B). However, in the presence of low concentrations of DLTIII, many of the ice discs had one or more indentations on their surface and formed highly irregular shapes (Figure 5C).

DOI: 10.1021/acs.bioconjchem.5b00290
Bioconjugate Chem. 2015, 26, 1908−1915

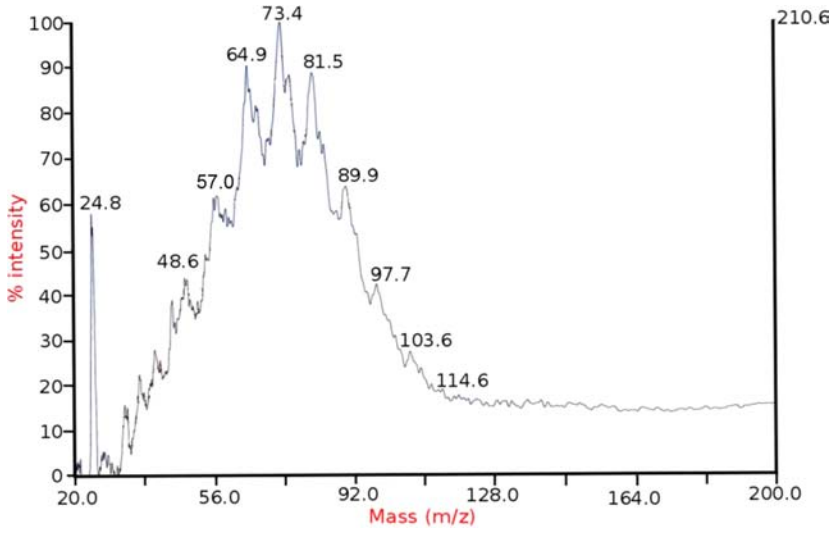

Figure 3. Analysis of the amount of cross-linking between G2-PAMAM dendrimer and type III A65C antifreeze protein. MALDI-TOF analysis of the purified product from the cross-linking reaction between the G2-PAMAM dendrimer and type III A65C.

Table 1. Estimation of the Amount of Type III A65C Antifreeze Proteins Attached to the G2-PAMAM Dendrimer

no. of type III[a]	predicted MW (kDa)	observed MW (kDa)
6	57.2	57.0
7	65.3	64.9
8	73.5	73.4
9	81.7	81.5
10	89.8	89.9
11	98.0	97.7
12	106.1	103.6

[a]Number of type III A65C attached is based on the proximity of the predicted molecular weight to the observed (MALDI) molecular weight.

DISCUSSION

By attaching multiple antifreeze proteins to the outward-pointing termini of a dendrimer, we were able to enhance both the AFP's TH and IRI activities. This was particularly evident at low multimer concentrations. Introducing a Cys into the AFP at a specific location in the known crystal structure and the use of a bifunctional cross-linker gave control over how the AFP was presented on the dendrimer surface, with its compound ice-binding site outermost to make first contact with ice.[25]

In the presence of DLTIII constructs, ice was shaped into a hexagonal bipyramid that burst along the *c*-axis, characteristic of type III AFP. This indicates that DLTIII binds to ice in a similar manner as that of monomeric type III and that any changes in activity are not due to changes in the planes of ice to which the AFP is binding. Furthermore, comparisons on a molar basis show a substantial increase in TH activity with DLTIII over that of monomeric type III. As the amount of DLTIII increases, its TH activity resembles a rectangular hyperbola curve. We think this increase in activity is due to the DLTIII having a greater impact on the ice surface due to both its larger size and faster binding. Additionally, if one compares the activity of DLTIII to monomeric type III AFP on a per AFP-domain basis, then DLTIII has slightly lower activity below 0.15 mM, but it has enhanced activity at concentrations greater than this value (Figure 4B). Similar to AFPs with an

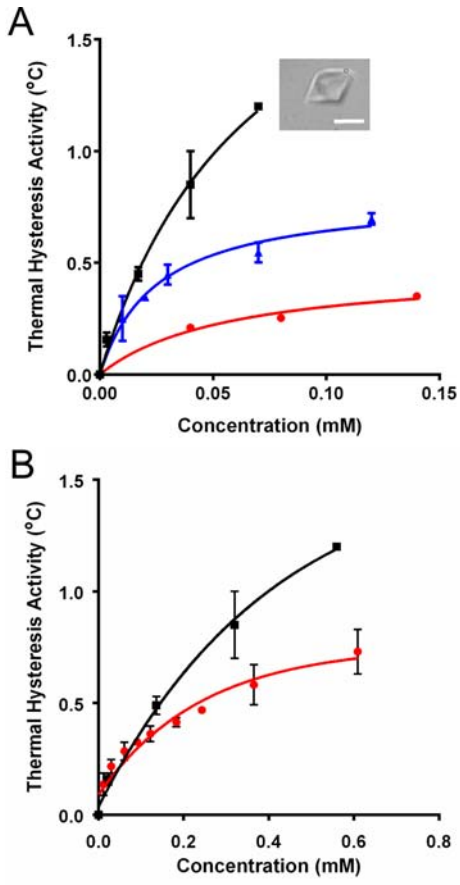

Figure 4. Assessment of the thermal hysteresis activity of the dendrimer-linked type III AFP molecule. (A) Comparison of TH activity on a molar basis of DLTIII molecules (black squares), type III AFP attached to maltose-binding protein (blue triangles), and monomeric type III A65C AFP (red dots). Inset: hexagonal bipyramid ice crystal formed in the presence of DLTIII. The white scale bar represents 10 μm. (B) Comparison of TH activity on a per AFP-domain basis. DLTIII conjugate (black squares) vs monomeric type III AFP (red dots). Here, the DLTIII concentration based on AFP content is 8 times greater than that used in (A).

DOI: 10.1021/acs.bioconjchem.5b00290
Bioconjugate Chem. 2015, 26, 1908−1915

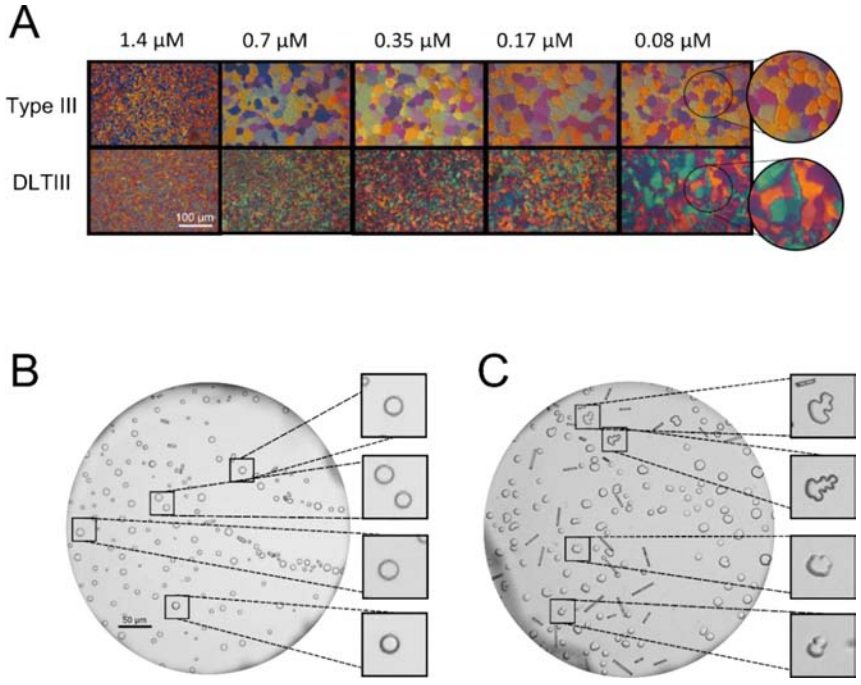

Figure 5. Assessment of IRI activity of dendrimer-linked type III AFP compared to monomeric type III AFP. (A) Splat assay results of type III AFP and DLTIII at various concentrations. Below: sucrose-sandwich IRI analysis of DLTIII. (B) Positive control for sucrose-sandwich RI assay. (C) Sucrose-sandwich assay of 0.14 μM DLTIII. Needle-shaped crystals are flat disks lying on their side rather than floating, with their round basal plane uppermost.

extended IBS, one advantage of having multiple IBSs is the ability to arrange a quorum of ice-like waters, facilitating the binding to ice.[17,18] By having multiple IBSs connected together, the minimum number of ice-like waters required to bind to ice could potentially be reached sooner, increasing the odds of a productive interaction between an AFP and a growing seed ice crystal and thereby leading to increased TH activity. Additionally, growth out of the basal plane might be restricted better by the large size of the DLTIII molecule binding at the edge of the basal−pyramidal plane.

It is generally accepted that TH caused by AFPs is due to the Kelvin effect.[1,26] When an AFP binds ice, water can only add to a growing ice crystal between ice-bound AFPs. This leads to a microcurvature of the ice and makes it energetically unfavorable for more water molecules to be incorporated into the ice and thus leads to a halting of growth. The distance between ice-bound AFPs has been measured only indirectly but will be a key piece of information in the future to guide further enhancements of AFP activity.[27] When one type III AFP attached to an arm of the dendrimer binds to ice, the likelihood that another type III AFP will be attached to the same dendrimer binding nearby will be increased. In this instance, how does the distance between these bound AFPs linked via the dendrimer compare to the distance between monomeric AFPs on the ice and between whole multimers? Dendrimers and two-dimensional branched polymers with AFPs attached could provide opportunities to control and change the distance between AFPs that are bound to ice to study this variable in relation to TH. We think that only a few (2 or 3) of the cross-linked type III AFPs in the DLTIII molecule are likely to bind to a single ice crystal due to the curvature of the dendrimer (Figure 6A). Higher-generation dendrimers with a larger radius and more reactive termini should have proportionally more AFPs bound to the matrix and therefore more AFPs on the same plane to contact ice. Two-dimensional arrays have the potential for full engagement of the bound AFPs.

In addition to an increase in TH activity, we hypothesized that we would see an increase in IRI activity due to the DLTIII construct potentially being able to bind to multiple ice crystals. The DLTIII molecule was equally effective as free type III AFP on a per AFP basis, but it was roughly 8 times better on a molar basis than monomeric type III at preventing ice recrystallization. We interpret the increased IRI activity compared to TH activity due to more AFPs of the DTLIII molecule being able to interact with ice (Figure 6B). In this two-dimensional model, DTLIII is shown interacting with four different ice crystal grains. In three dimensions, the possibilities for interacting with multiple ice grains are enhanced.

The DLTIII molecule has been modeled to be roughly spherical with ice-binding sites of type III AFP molecules facing outward in all directions (Supporting Information Figure S1). It is thought, when ice recrystallization occurs in the absence of sufficient AFPs, that smaller ice crystals melt and the liberated water joins a nearby larger ice crystal to further increase the latter's size. Dendrimers might simultaneously interact with different sized ice grains; AFPs on one part of the dendrimer could be preventing an ice grain from getting bigger by freezing point depression while preventing another grain from getting smaller by raising the melting point (melting hysteresis). Also, the large size of the DLTIII complex should resist engulfment better than a single type III AFP and thus help to maintain a high effective AFP concentration in the intergrain boundary regions. Irregularly shaped ice grain boundaries seen in Figure 5A in the presence of DLTIII might result from two or more ice crystals being bound together such that when a smaller ice crystal begins to melt it pulls on the DLTIII molecule, inducing a stress on the other ice crystal. The ability of the DLTIII molecule to simultaneously bind multiple ice crystals and the

DOI: 10.1021/acs.bioconjchem.5b00290
Bioconjugate Chem. 2015, 26, 1908−1915

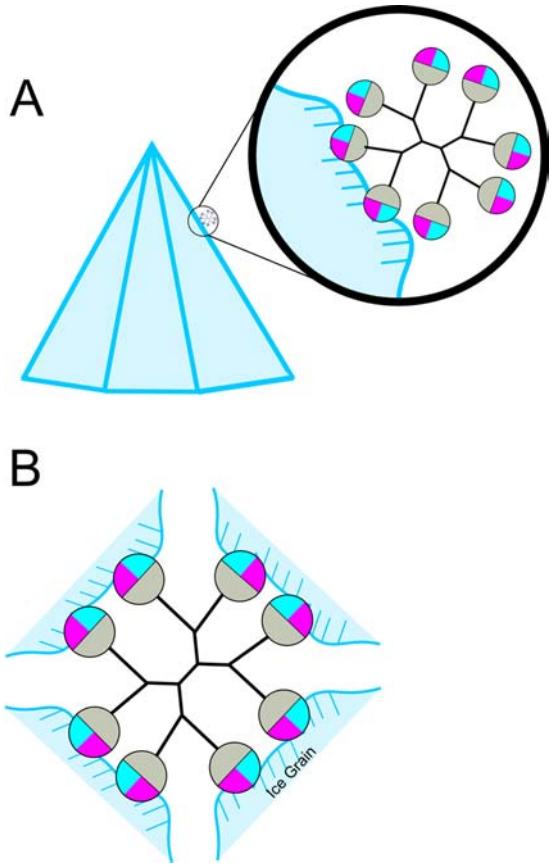

Figure 6. Schematic representation of DLTIII binding ice. (A) DTLIII binding to a single ice crystal, as in thermal hysteresis experiments. (B) DLTIII simultaneously binding several ice crystals, which may occur during ice recrystallization. The compound ice-binding site of type III AFP is colored in purple (pyramidal plane) and cyan (prism plane). The dendrimer is shown as branched lines, and the ice grain surfaces are marked by hatched line. This is a two-dimensional representation of a binding relationship that will occur in three dimensions.

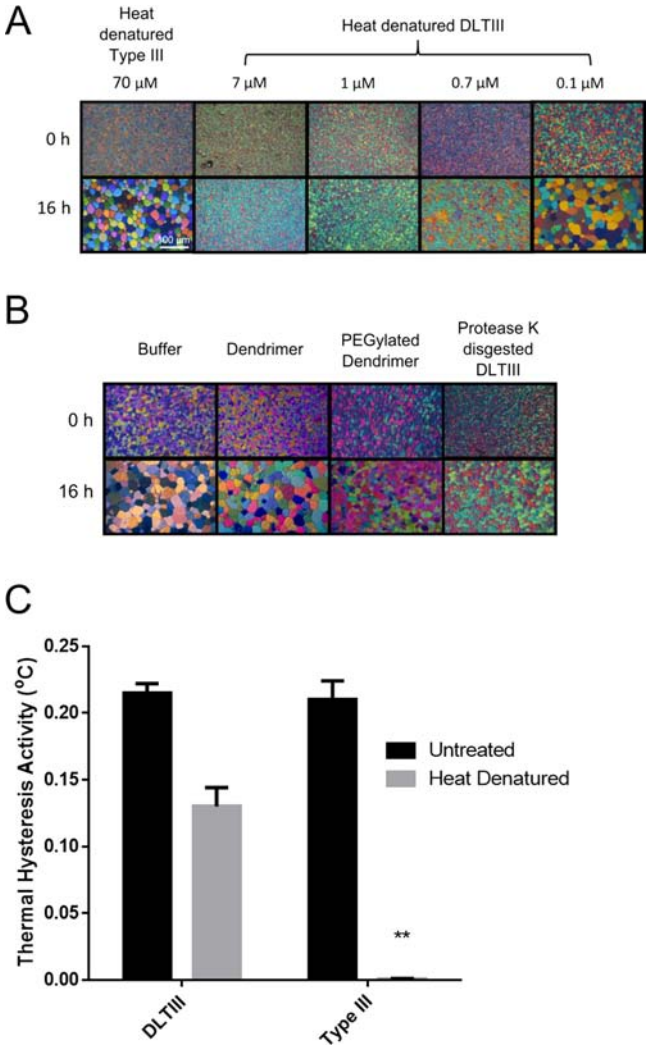

Figure 7. Assessment of IRI and TH activities of type III and DLTIII after heat denaturation. Samples of type III AFP and DLTIII were heated in boiling water for 30 min and then cooled rapidly to 4 °C. (A) The IRI ability of various concentrations of heat-denatured type III and DLTIII was investigated by the splat-cooling assay. (B) IRI assay controls consisting of buffer (50 mM HEPES pH 8.4, 20 mM NaCl), 2.7 mM G2-PAMAM dendrimer, 54 μM PEGylated dendrimer (SM(PEG)2 modified dendrimer), and DLTIII boiled and then digested with Protease K. (C) TH activity of 7 μM DLTIII and 70 μM type III AFP was examined before and after the heat-denaturing protocol. Double asterisk denotes that monomeric type III was tested but had zero activity.

increased local concentration of AFPs lead to superior IRI activities. Furthermore, higher-generation dendrimers may potentially lead to more effective molecules for the control of ice growth. Higher-generation dendrimers have more arms available for AFP attachment, which may lead to an increase in activity through the larger particle size and more AFPs available to bind to an ice plane.

Another interesting innovation attained from attaching type III AFPs to a dendrimer is resistance to, or recovery from, heat denaturation (Figure 7). We think type III AFPs linked to the dendrimer unfold when subjected to boiling temperatures. However, due to the high solubility of the dendrimer and PEG cross-linker, type III AFP is prevented from aggregating by being physically restrained at one end and by being given a longer opportunity to refold without aggregation over that of monomeric type III. It is clear from the 50% reduction in activity that not every type III AFP is able to recover from thermal insult (Figure 7C). However, this encouraging result has potential for many applications in medicine or food preservation, where there is a requirement for sterilization before use.

Generating AFP constructs with enhanced activities will provide superior reagents for cold storage and cryopreservation systems. Here, we have combined two approaches to achieve this goal. With the use of higher-order dendrimers, hyperactive AFPs, and optimizing the density of conjugation, greater increases in antifreeze activity can be potentially achieved.

EXPERIMENTAL SECTION

Type III A65C Protein Expression and Purification. The A65C mutant of type III AFP from the m1.1 clone in pET 20b with a C-terminal His-tag was generated by primer-directed mutagenesis using the primer sequence 5′-GTTAAAGGTTA-CGCTTGTCTCGAGCACCAC-3′.[28] The terminal Ala in the altered C-terminal YAA sequence was changed to Cys. Protein preparation was performed as detailed by Baardsnes et al. with slight changes.[16] Cells were pelleted by centrifugation at 3000*g* in a Beckman Coulter JS 4.2 rotor and resuspended in 25 mL of

DOI: 10.1021/acs.bioconjchem.5b00290
Bioconjugate Chem. 2015, 26, 1908−1915

buffer N (50 mM Tris-HCl (pH 7.6), 200 mM NaCl, 5 mM imidazole, 100 μL PMSF). Ni^{2+}-NTA fractions totaling approximately 20 mL were diluted to 100 mL in no-salt buffer A (50 mM Tris-HCl (pH 7.6)) and subjected to cation-exchange chromatography on a High-Load 16/10 Q-Sepharose high-performance column (GE Healthcare). The purity of various column fractions was assessed by SDS-PAGE on a 10% (w/v) gel. Fractions containing AFP alone were pooled and concentrated to 7 mg/mL, as determined by UV absorbance using the protein's extinction coefficient as predicted by ProtParam (http://web.expasy.org/protparam/). This concentrated protein was stored in reducing storage buffer (50 mM Tris-HCl (pH 7.6), 50 mM NaCl, 5 mM TCEP).

Conjugating Type III AFP to Dendrimer. Second-generation polyamidoamine (PAMAM) dendrimer (Dendritech) was diluted to 27 μM in conjugation buffer (50 mM Hepes (pH 8.4), 50 mM NaCl) to a final volume of 1 mL. The diluted dendrimer was reacted with 20 μL of 250 mM $SM(PEG)_2$ cross-linker (ThermoFisher) for 1 h at room temperature with mixing. Unreacted cross-linker was separated from the conjugated sample using a Sephadex G-10 desalting spin column (GE Healthcare). Reduced type III A65C was buffer-exchanged into conjugation buffer using a centricon 3 kDa molecular weight cutoff centrifugal filter (GE Healthcare). In a 15 mL Falcon tube, 35 mg of reduced type III A65C was reacted with approximately 1 mL of cross-linker-modified dendrimer with mixing at room temperature for 4 h and then overnight at 4 °C. The products resulting from conjugation were fractionated by gel-permeation chromatography using a G-75 column (Amersham Biosciences) equilibrated in 50 mM Tris-HCl (pH 8) and 50 mM NaCl. Conjugation efficiency and purity were assessed by 10% Tris-tricine SDS-PAGE with β-propionic acid and New England BioLabs broad range protein marker (2−212 kDa). After purification, DLTIII was concentrated to form a stock solutions. The amount of type III AFP conjugated to the dendrimer was determined by amino acid analysis and confirmed by UV−vis A_{280} readings using ABS 1.0% (mg/mL) = 1.82. Dilutions of the stock solution were used in TH and IRI experiments.

Thermal Hysteresis Assay. TH assays were performed as previously described, with slight modifications.[29] TH measurements were performed in 50 mM Tris-HCl (pH 8) and 50 mM NaCl. The temperature was decreased at rate of 0.01 °C/min. Samples were cooled by a Clifton nanoliter stage driven by LabView program via a 3040 temperature controller (Newport). Images were recorded using a Panasonic WV-BL200 digital camera at a rate of 30 fps. TH values were measured in triplicate at each concentration with the exception of 0.07 mM due to high amounts of melting hysteresis. Average ice crystal size tested was 20 μm.

Sucrose Sandwich IRI Assay. Sucrose sandwich IRI assays were performed as described by Smallwood et al.[30,31] Briefly, protein samples in a buffer (20 mM Tris-HCl, pH 7.6) containing 45% sucrose were sandwiched between two coverslips, and the edges were sealed with grease. Samples were cooled to, and held at, −50 °C for 2 min on a Linkam MDBCS 196 temperature-controlled cold stage (Linkam Scientific Instruments). The temperature was then elevated to −6 °C and held for 2 h. During this time, images were recorded every minute (QImaging EXi Aqua bio-imaging microscopy camera).

Splat Cooling IRI Assay. Splat cooling assays were performed as previously described by Tomczak et al.[32] Briefly, a 10 μL aliquot of sample in 150 mM NaCl containing 10 mM Tris-HCl (pH 7.5) was dropped from ∼1 m onto a polished metal block precooled to −78 °C by solid carbon dioxide. The resulting splat (ice wafer) was transferred to a cooling bath of 2,2,4-trimethylpentane maintained at −6 °C for 16 h. The ice wafers were photographed with a Canon EDOS 50S camera between two crossed polarizers to determine changes in ice crystal grain size.

Heat Denaturation. Samples (0.5 mL) in 1.5 mL Eppendorf tubes were heated in boiling water for 30 min and then rapidly cooled by transfer to wet ice.

Modeling of Dendrimer Fully Loaded with Type III AFP. G2 PAMAM dendrimer, SM(PEG)2 cross-linker, and cross-linker-modified dendrimer molecules were built using PyMOL (Schrödinger, 2010). A topology file of the cross-linker-modified dendrimer molecule was generated using SwissParam. Paired with Gromacs, the topology file was used to construct an energy-minimized version of the cross-linker-modified dendrimer. To the energy-minimized structure were bonded multiple copies of type III AFP (PDB ID: 1HG7); no further energy minimization was done.

Predicted Dendrimer-Linked Type III Mass and Concentration. The predicted mass of a dendrimer linked to eight AFP molecules was calculated based on the assumption that the G2-PAMAM dendimer (3.256 kDa) was fully modified with 16 cross-linkers (0.31 kDa each). Then the mass of eight type III AFPs (8 × 8.132 kDa) was added to the cross-linker-modified dendrimer's mass (8.216 kDa). The observed mass was determined using a Sciex DE Pro MALDI-TOF. The DLTIII sample was desalted using C4 zip tips and ionized by sinapinic acid matrix. The molarity of a DLTIII solution was calculated based on the amount of protein determined from amino acid analysis and the mean molecular weight of eight type III AFPs linked to the dendrimer (73.4 kDa).

■ ASSOCIATED CONTENT

Supporting Information

The Supporting Information is available free of charge on the ACS Publications website at DOI: 10.1021/acs.bioconjchem.5b00290.

Thermal hysteresis controls and ice shaping for heat denaturation experiments; linear regression analysis of MALDI-TOF masses (PDF).

A rotating model demonstrating the three-dimensonal nature of the dendrimer-linked type III AFP molecule (AVI).

■ AUTHOR INFORMATION

Corresponding Author

*E-mail: peter.davies@queensu.ca.

Notes

The authors declare no competing financial interest.

■ ACKNOWLEDGMENTS

P.L.D holds the Canada Research Chair in Protein Engineering. This work was funded by a grant from the Canadian Institutes of Health Research and was facilitated by a Lady Davis Fellowship awarded to P.L.D. This work was also supported by a European Research Council award to I.B. C.A.S. recognizes support from a R.S. McLaughlin Scholarship as well as a Queen's Doctoral Field Travel Grant. The authors would like

DOI: 10.1021/acs.bioconjchem.5b00290
Bioconjugate Chem. 2015, 26, 1908−1915

to thank Sherry Gauthier, Laurie Graham, and Rob Campbell for their technical assistance.

■ ABBREVIATIONS

AFP, antifreeze protein; G2-PAMAM, second-generation polyamidoamine; TH, thermal hysteresis; IRI, ice recrystallization inhibition; NHS, *N*-hydroxysuccinimide; PEG, poly(ethylene glycol); DLTIII, dendrimer-linked type III antifreeze protein; IBS, ice-binding site

■ REFERENCES

(1) Davies, P. L. (2014) Ice-binding proteins: a remarkable diversity of structures for stopping and starting ice growth. *Trends Biochem. Sci. 39*, 548−55.
(2) Griffith, M., and Yaish, M. W. (2004) Antifreeze proteins in overwintering plants: a tale of two activities. *Trends Plant Sci. 9*, 399−405.
(3) Regand, A., and Goff, H. D. (2006) Ice recrystallization inhibition in ice cream as affected by ice structuring proteins from winter wheat grass. *J. Dairy Sci. 89*, 49−57.
(4) Soltys, K. A., Batta, A. K., and Koneru, B. (2001) Successful nonfreezing, subzero preservation of rat liver with 2,3-butanediol and type I antifreeze protein. *J. Surg. Res. 96*, 30−4.
(5) Amir, G., Rubinsky, B., Basheer, S. Y., Horowitz, L., Jonathan, L., Feinberg, M. S., Smolinsky, A. K., and Lavee, J. (2005) Improved viability and reduced apoptosis in sub-zero 21-h preservation of transplanted rat hearts using anti-freeze proteins. *Journal of heart and lung transplantation 24*, 1915−29.
(6) Carpenter, J. F., and Hansen, T. N. (1992) Antifreeze protein modulates cell survival during cryopreservation: mediation through influence on ice crystal growth. *Proc. Natl. Acad. Sci. U. S. A. 89*, 8953−7.
(7) Arav, A., Rubinsky, B., Fletcher, G., and Seren, E. (1993) Cryogenic protection of oocytes with antifreeze proteins. *Mol. Reprod. Dev. 36*, 488−93.
(8) Capicciotti, C. J., Kurach, J. D., Turner, T. R., Mancini, R. S., Acker, J. P., and Ben, R. N. (2015) Small molecule ice recrystallization inhibitors enable freezing of human red blood cells with reduced glycerol concentrations. *Sci. Rep. 5*, 9692.
(9) Heisig, M., Mattessich, S., Rembisz, A., Acar, A., Shapiro, M., Booth, C. J., Neelakanta, G., and Fikrig, E. (2015) Frostbite protection in mice expressing an antifreeze glycoprotein. *PLoS One 10*, e0116562.
(10) Halwani, D. O., Brockbank, K. G., Duman, J. G., and Campbell, L. H. (2014) Recombinant Dendroides canadensis antifreeze proteins as potential ingredients in cryopreservation solutions. *Cryobiology 68*, 411−8.
(11) Balogh, L. P. (2007) Dendrimer 101. *Adv. Exp. Med. Biol. 620*, 136−155.
(12) Tomalia, D. A., Naylor, A. M., and Goddard, W. A. (1990) Starburst Dendrimers - Molecular-Level Control of Size, Shape, Surface-Chemistry, Topology, and Flexibility from Atoms to Macroscopic Matter. *Angew. Chem., Int. Ed. Engl. 29*, 138−75.
(13) Esfand, R., and Tomalia, D. A. (2001) Poly(amidoamine) (PAMAM) dendrimers: from biomimicry to drug delivery and biomedical applications. *Drug Discovery Today 6*, 427−436.
(14) Nanaware-Kharade, N., Gonzalez, G. A., 3rd, Lay, J. O., Jr., Hendrickson, H. P., and Peterson, E. C. (2012) Therapeutic anti-methamphetamine antibody fragment-nanoparticle conjugates: synthesis and in vitro characterization. *Bioconjugate Chem. 23*, 1864−72.
(15) DeLuca, C. I., Comley, R., and Davies, P. L. (1998) Antifreeze proteins bind independently to ice. *Biophys. J. 74*, 1502−8.
(16) Baardsnes, J., Kuiper, M. J., and Davies, P. L. (2003) Antifreeze protein dimer: when two ice-binding faces are better than one. *J. Biol. Chem. 278*, 38942−7.
(17) Marshall, C. B., Daley, M. E., Sykes, B. D., and Davies, P. L. (2004) Enhancing the activity of a beta-helical antifreeze protein by the engineered addition of coils. *Biochemistry 43*, 11637−46.
(18) Leinala, E. K., Davies, P. L., Doucet, D., Tyshenko, M. G., Walker, V. K., and Jia, Z. (2002) A beta-helical antifreeze protein isoform with increased activity. Structural and functional insights. *J. Biol. Chem. 277*, 33349−52.
(19) Nishimiya, Y., Ohgiya, S., and Tsuda, S. (2003) Artificial multimers of the type III antifreeze protein. Effects on thermal hysteresis and ice crystal morphology. *J. Biol. Chem. 278*, 32307−12.
(20) Can, O., and Holland, N. B. (2013) Utilizing avidity to improve antifreeze protein activity: a type III antifreeze protein trimer exhibits increased thermal hysteresis activity. *Biochemistry 52*, 8745−52.
(21) Congdon, T., Notman, R., and Gibson, M. I. (2013) Antifreeze (glyco)protein mimetic behavior of poly(vinyl alcohol): detailed structure ice recrystallization inhibition activity study. *Biomacromolecules 14*, 1578−86.
(22) Wang, H. Y., Inada, T., Funakoshi, K., and Lu, S. S. (2009) Inhibition of nucleation and growth of ice by poly(vinyl alcohol) in vitrification solution. *Cryobiology 59*, 83−9.
(23) Bar-Dolev, M., Celik, Y., Wettlaufer, J. S., Davies, P. L., and Braslavsky, I. (2012) New insights into ice growth and melting modifications by antifreeze proteins. *J. R. Soc., Interface 9*, 3249−59.
(24) Celik, Y., Graham, L. A., Mok, Y. F., Bar, M., Davies, P. L., and Braslavsky, I. (2010) Superheating of ice crystals in antifreeze protein solutions. *Proc. Natl. Acad. Sci. U. S. A. 107*, 5423−8.
(25) Garnham, C. P., Natarajan, A., Middleton, A. J., Kuiper, M. J., Braslavsky, I., and Davies, P. L. (2010) Compound ice-binding site of an antifreeze protein revealed by mutagenesis and fluorescent tagging. *Biochemistry 49*, 9063−71.
(26) Raymond, J. A., and DeVries, A. L. (1977) Adsorption inhibition as a mechanism of freezing resistance in polar fishes. *Proc. Natl. Acad. Sci. U. S. A. 74*, 2589−93.
(27) Drori, R., Davies, P. L., and Braslavsky, I. (2015) Experimental correlation between thermal hysteresis activity and the distance between antifreeze proteins on an ice surface. *RSC Adv. 5*, 7848−7853.
(28) Chao, H., Davies, P. L., Sykes, B. D., and Sonnichsen, F. D. (1993) Use of proline mutants to help solve the NMR solution structure of type III antifreeze protein. *Protein Sci. 2*, 1411−28.
(29) Braslavsky, I., and Drori, R. (2013) LabVIEW-operated novel nanoliter osmometer for ice binding protein investigations. *J. Visualized Exp.*, e4189.
(30) Smallwood, M., Worrall, D., Byass, L., Elias, L., Ashford, D., Doucet, C. J., Holt, C., Telford, J., Lillford, P., and Bowles, D. J. (1999) Isolation and characterization of a novel antifreeze protein from carrot (Daucus carota). *Biochem. J. 340*, 385−91.
(31) Kumble, K. D., Demmer, J., Fish, S., Hall, C., Corrales, S., DeAth, A., Elton, C., Prestidge, R., Luxmanan, S., Marshall, C. J., et al. (2008) Characterization of a family of ice-active proteins from the Ryegrass, Lolium perenne. *Cryobiology 57*, 263−8.
(32) Tomczak, M. M., Marshall, C. B., Gilbert, J. A., and Davies, P. L. (2003) A facile method for determining ice recrystallization inhibition by antifreeze proteins. *Biochem. Biophys. Res. Commun. 311*, 1041−6.

DOI: 10.1021/acs.bioconjchem.5b00290
Bioconjugate Chem. 2015, 26, 1908−1915